Dear Author,

Here are the proofs of your article.

- You can submit your corrections **online**, via **e-mail** or by **fax**.
- For **online** submission please insert your corrections in the online correction form. Always indicate the line number to which the correction refers.
- You can also insert your corrections in the proof PDF and **email** the annotated PDF.
- For fax submission, please ensure that your corrections are clearly legible. Use a fine black pen and write the correction in the margin, not too close to the edge of the page.
- Remember to note the **journal title**, **article number**, and **your name** when sending your response via e-mail or fax.
- **Check** the metadata sheet to make sure that the header information, especially author names and the corresponding affiliations are correctly shown.
- **Check** the questions that may have arisen during copy editing and insert your answers/ corrections.
- **Check** that the text is complete and that all figures, tables and their legends are included. Also check the accuracy of special characters, equations, and electronic supplementary material if applicable. If necessary refer to the *Edited manuscript.*
- The publication of inaccurate data such as dosages and units can have serious consequences. Please take particular care that all such details are correct.
- Please **do not** make changes that involve only matters of style. We have generally introduced forms that follow the journal's style. Substantial changes in content, e.g., new results, corrected values, title and authorship are not allowed without the approval of the responsible editor. In such a case, please contact the Editorial Office and return his/her consent together with the proof.
- If we do not receive your corrections **within 48 hours**, we will send you a reminder.
- Your article will be published **Online First** approximately one week after receipt of your corrected proofs. This is the **official first publication** citable with the DOI. **Further changes are, therefore, not possible.**
- The **printed version** will follow in a forthcoming issue.

Please note

After online publication, subscribers (personal/institutional) to this journal will have access to the complete article via the DOI using the URL: http://dx.doi.org/[DOI].
If you would like to know when your article has been published online, take advantage of our free alert service. For registration and further information go to: http://www.link.springer.com.

Due to the electronic nature of the procedure, the manuscript and the original figures will only be returned to you on special request. When you return your corrections, please inform us if you would like to have these documents returned.

Metadata of the article that will be visualized in OnlineFirst

ArticleTitle	Parametric Study on PVDF Electrospun Nanofibers: Optical Characteristics, Piezoelectric Analysis, and Correlated Applications	
Article Sub-Title		
Article CopyRight	The Minerals, Metals & Materials Society (This will be the copyright line in the final PDF)	
Journal Name	Journal of Electronic Materials	
Corresponding Author	FamilyName	**Nair**
	Particle	
	Given Name	**Remya**
	Suffix	
	Division	School of Applied Sciences
	Organization	Suresh Gyan Vihar University Jaipur
	Address	Jaipur, India
	Division	
	Organization	Kuwait College of Science and Technology
	Address	Doha Area, 7th Ring Road, 13133, Safat, Kuwait
	Phone	
	Fax	
	Email	r.nair@kcst.edu.kw
	URL	
	ORCID	
Author	FamilyName	**Mahdi**
	Particle	
	Given Name	**Jaffer**
	Suffix	
	Division	
	Organization	Kuwait College of Science and Technology
	Address	Doha Area, 7th Ring Road, 13133, Safat, Kuwait
	Phone	
	Fax	
	Email	
	URL	
	ORCID	
Author	FamilyName	**Amjad**
	Particle	
	Given Name	**Omar**
	Suffix	
	Division	
	Organization	Kuwait College of Science and Technology
	Address	Doha Area, 7th Ring Road, 13133, Safat, Kuwait
	Phone	
	Fax	
	Email	
	URL	
	ORCID	
Author	FamilyName	**Maree**
	Particle	
	Given Name	**Kareem**
	Suffix	
	Division	
	Organization	Kuwait College of Science and Technology
	Address	Doha Area, 7th Ring Road, 13133, Safat, Kuwait
	Phone	
	Fax	
	Email	
	URL	
	ORCID	

Author	FamilyName	**Jain**
	Particle	
	Given Name	**Ankur**
	Suffix	
	Division	Centre for Renewable Energy and Storage
	Organization	Suresh Gyan Vihar University
	Address	Jaipur, India
	Phone	
	Fax	
	Email	ankur.j.ankur@gmail.com
	URL	
	ORCID	
Author	FamilyName	**Al-Dubai**
	Particle	
	Given Name	**Ahmed**
	Suffix	
	Division	School of Engineering and the Built Environment
	Organization	Edinburgh Napier University
	Address	Edinburgh, EH10 5DT, UK
	Phone	
	Fax	
	Email	
	URL	
	ORCID	
Author	FamilyName	**Jaradat**
	Particle	
	Given Name	**Suha**
	Suffix	
	Division	School of Engineering and the Built Environment
	Organization	Edinburgh Napier University
	Address	Edinburgh, EH10 5DT, UK
	Phone	
	Fax	
	Email	
	URL	
	ORCID	
Author	FamilyName	**Shyha**
	Particle	
	Given Name	**Islam**
	Suffix	
	Division	School of Engineering and the Built Environment
	Organization	Edinburgh Napier University
	Address	Edinburgh, EH10 5DT, UK
	Phone	
	Fax	
	Email	
	URL	
	ORCID	
Author	FamilyName	**Trabelsi**
	Particle	
	Given Name	**Mohamed**
	Suffix	
	Division	
	Organization	Kuwait College of Science and Technology
	Address	Doha Area, 7th Ring Road, 13133, Safat, Kuwait
	Phone	
	Fax	
	Email	
	URL	
	ORCID	

Author	FamilyName	**Alothamn**
	Particle	
	Given Name	**Basil**
	Suffix	
	Division	
	Organization	Kuwait College of Science and Technology
	Address	Doha Area, 7th Ring Road, 13133, Safat, Kuwait
	Phone	
	Fax	
	Email	
	URL	
	ORCID	
Author	FamilyName	**Shehata**
	Particle	
	Given Name	**Nader**
	Suffix	
	Division	
	Organization	Kuwait College of Science and Technology
	Address	Doha Area, 7th Ring Road, 13133, Safat, Kuwait
	Division	School of Engineering and the Built Environment
	Organization	Edinburgh Napier University
	Address	Edinburgh, EH10 5DT, UK
	Division	Center of Smart Materials, Nanotechnology and Photonics (CSMNP), Smart CI Research Center
	Organization	Alexandria University
	Address	Alexandria, 21544, Egypt
	Division	Department of Engineering Mathematics and Physics, Faculty of Engineering
	Organization	Alexandria University
	Address	Alexandria, 21544, Egypt
	Division	USTAR Bioinnovations Center, Faculty of Science
	Organization	Utah State University
	Address	Logan, UT, 84341, USA
	Division	School of Engineering
	Organization	Ulster University
	Address	Belfast, BT15 1AP, UK
	Phone	
	Fax	
	Email	n.shehata@kcst.edu.kw; n.shehata@ulster.ac.uk
	URL	
	ORCID	

Schedule	Received	4 Nov 2023
	Revised	
	Accepted	4 Apr 2024

Abstract	In this study, both the optical and piezoelectric properties of polyvinylidene fluoride (PVDF) electrospun nanofibers were investigated at different needle-to-collector distances of the electrospinning process at constant applied high voltage. For piezoelectric characterization, the fabricated nanofiber mats were subjected to applied forces, including cyclic force, variable frequency-based loads, and free-falling masses (impulse loading), along with power density analysis for different load resistance values. In addition, both optical absorbance and transmittance measurements were conducted to evaluate the optical properties of the fabricated nanofibers. The piezoelectric analysis demonstrated the best piezoresponse of the fabricated nanomats at a needle-to-collector distance of 15 cm and high voltage of 22 kV. However, a trade-off between piezoelectric response and optical transmissivity was observed based on the electrospinning distance parameter. The relatively higher optically transparent sample exhibited only moderate piezoelectric response, while the less transparent sample displayed the highest piezoelectric activity. Based on the optimized sample and piezoelectric analysis, the synthesized nanofiber mat was subjected to applied mechanical stress in the form of variable velocity and momentum loads. A maximum potential of approximately 16 V was harvested through velocity and momentum impact, especially with the addition of a double-layer PVDF membrane. Furthermore, the sensing effect of airflow pressure on single/double-layer PVDF was studied. The single-layer PVDF membrane generated 79 mV under an airflow speed of 21 km/h, while the double-layer membrane produced 114 mV potential under the same airflow. This study highlights the diverse applications of PVDF nanofiber mats as multifunctional sensors and energy harvesting applications from mechanical shocks and airflow impact.

Keywords (separated by '-')	Piezoelectric energy harvesting - electroactivity - nanofibers - sensors - nanotechnology - nanogenerator - transduction
Footnote Information	

Journal of Electronic Materials
https://doi.org/10.1007/s11664-024-11097-7

ORIGINAL RESEARCH ARTICLE

Parametric Study on PVDF Electrospun Nanofibers: Optical Characteristics, Piezoelectric Analysis, and Correlated Applications

Remya Nair[1,2] · Jaffer Mahdi[2] · Omar Amjad[2] · Kareem Maree[2] · Ankur Jain[3] · Ahmed Al-Dubai[4] · Suha Jaradat[4] · Islam Shyha[4] · Mohamed Trabelsi[2] · Basil Alothamn[2] · Nader Shehata[2,4,5,6,7,8]

Received: 4 November 2023 / Accepted: 4 April 2024

Abstract

In this study, both the optical and piezoelectric properties of polyvinylidene fluoride (PVDF) electrospun nanofibers were investigated at different needle-to-collector distances of the electrospinning process at constant applied high voltage. For piezoelectric characterization, the fabricated nanofiber mats were subjected to applied forces, including cyclic force, variable frequency-based loads, and free-falling masses (impulse loading), along with power density analysis for different load resistance values. In addition, both optical absorbance and transmittance measurements were conducted to evaluate the optical properties of the fabricated nanofibers. The piezoelectric analysis demonstrated the best piezoresponse of the fabricated nanomats at a needle-to-collector distance of 15 cm and high voltage of 22 kV. However, a trade-off between piezoelectric response and optical transmissivity was observed based on the electrospinning distance parameter. The relatively higher optically transparent sample exhibited only moderate piezoelectric response, while the less transparent sample displayed the highest piezoelectric activity. Based on the optimized sample and piezoelectric analysis, the synthesized nanofiber mat was subjected to applied mechanical stress in the form of variable velocity and momentum loads. A maximum potential of approximately 16 V was harvested through velocity and momentum impact, especially with the addition of a double-layer PVDF membrane. Furthermore, the sensing effect of airflow pressure on single/double-layer PVDF was studied. The single-layer PVDF membrane generated 79 mV under an airflow speed of 21 km/h, while the double-layer membrane produced 114 mV potential under the same airflow. This study highlights the diverse applications of PVDF nanofiber mats as multifunctional sensors and energy harvesting applications from mechanical shocks and airflow impact.

Keywords Piezoelectric energy harvesting · electroactivity · nanofibers · sensors · nanotechnology · nanogenerator · transduction

✉ Remya Nair
r.nair@kcst.edu.kw

Ankur Jain
ankur.j.ankur@gmail.com

Nader Shehata
n.shehata@kcst.edu.kw; n.shehata@ulster.ac.uk

[1] School of Applied Sciences, Suresh Gyan Vihar University Jaipur, Jaipur, India

[2] Kuwait College of Science and Technology, Doha Area, 7th Ring Road, 13133 Safat, Kuwait

[3] Centre for Renewable Energy and Storage, Suresh Gyan Vihar University, Jaipur, India

[4] School of Engineering and the Built Environment, Edinburgh Napier University, Edinburgh EH10 5DT, UK

[5] Center of Smart Materials, Nanotechnology and Photonics (CSMNP), Smart CI Research Center, Alexandria University, Alexandria 21544, Egypt

[6] Department of Engineering Mathematics and Physics, Faculty of Engineering, Alexandria University, Alexandria 21544, Egypt

[7] USTAR Bioinnovations Center, Faculty of Science, Utah State University, Logan, UT 84341, USA

[8] School of Engineering, Ulster University, Belfast BT15 1AP, UK

Introduction

Nanotechnology involves engineering active systems at a scale of 10^{-9} m, enhancing the surface-to-volume ratio and interatomic interaction. It is highly sought after in material science, industrial sectors, and research areas. Nanostructures such as nanoparticles, nanowires, nanofibers, and nanolayers have several fascinating properties that make them the foundation for any nanotechnology-based applications.[1–4] One-dimensional nanomaterials with nanoscale diameter or thickness, especially nanofibers, have been extensively studied due to their captivating properties such as excellent mechanical strength, high porosity with small pore size, easy reusability, and flexibility.[5,6] Nanofiber production involves natural and synthetic materials, with polymers being the most popular due to their flexibility, recyclability, low cost, and affordability. Techniques for fabrication include phase separation, template synthesis, drawing, electrospinning, and self-assembly. Advancements in polymer science and chemistry have led to the generation of synthetic nanofibers.[7] Electrospinning is the most cost-effective and simple method for developing efficient nanofibers. This non-interrupted process involves electrifying liquid droplets under a kilovolt electric potential, resulting in elongated and stretched jets, forming ultrathin, fine nanofibers as shown in Fig. 1. Electrostatic repulsion distorts droplets into Taylor cones, increasing surface area and suppressing repulsive forces. As voltage increases, the repulsive force becomes unstable, ejecting a charged jet from the conical drop tip.[8,9]

Electrospun nanofibers are in high demand due to their applications in filtration, smart textiles, protective clothing, cosmetics, sensors, energy harvesting, electrical, and biomedical fields.[10] A variety of piezo materials are studied for electrospun nanofibers, especially for application in the fields of sensing and energy harvesting. Polymers are a common alternative for piezoelectric conversion because of their versatility, low cost, variety of manufacturing techniques, light weight, and recyclability in comparison with other piezomaterials such as crystals and ceramics.[11,12]

The unique phenomenon known as piezoelectricity is the production of electrical energy from mechanical energy without the need for an external voltage input. The elemental structure connected to the crystal lattice is disrupted when an external mechanical force is applied to piezomaterials. The positive and negative charges are kept in a balanced equilibrium in the case of a typical crystalline structure. When a mechanical stress is applied, the balanced equilibrium is disturbed, leading to an uneven dipole configuration and the subsequent creation of electrical charge. This occurs by the deformation of the internal crystal structure and disruption of charge balance, and as a result, positive and negative charges are separated, and the neutrality of the material is destroyed. This phenomenon, referred to as spontaneous polarization, is caused by the displacement of electron

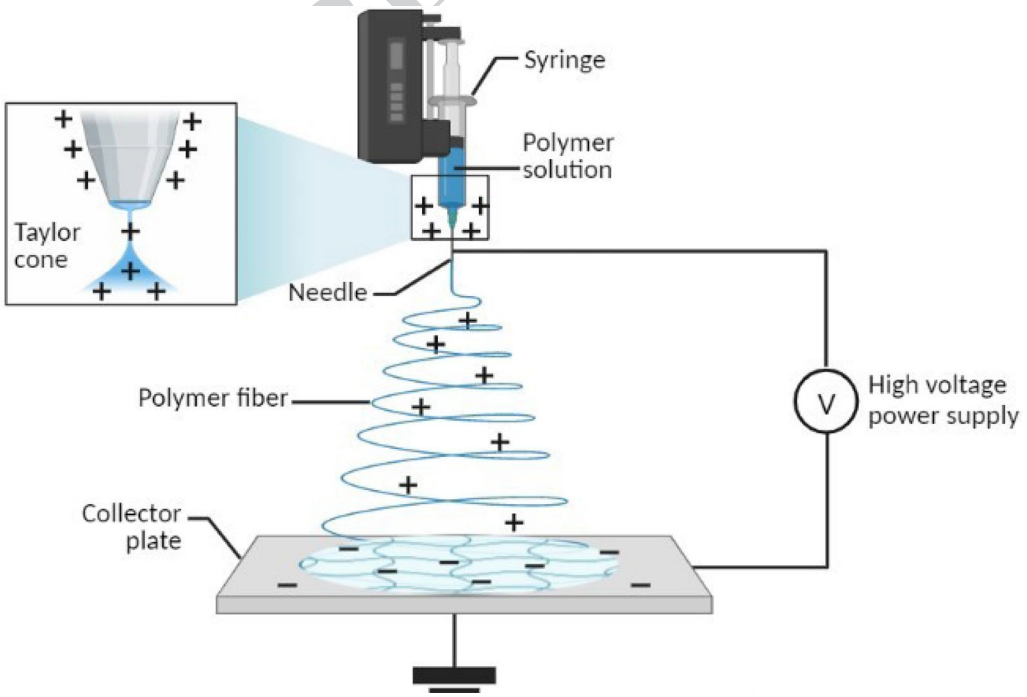

Fig. 1 Electrospinning experimental set up used for the fabrication of nanofiber membrane.

Journal : Large 11664 | Article No : 11097 | Pages : 18 | MS Code : 11097 | Dispatch : 29-4-2024

clouds relative to their individual atomic centers, that is, displacement of positive ions relative to negative ions within their crystal cells producing electric dipoles. The abovementioned displacement is called electric charge density displacement (D). The performance of a piezoelectric material mainly depends on the associated electric dipoles and their symmetry. Non-centrosymmetric crystals are more susceptible to the piezoelectric effect, and they exhibit piezoelectric responses upon application of an external mechanical stress. The reverse of this effect occurs when an applied electrical voltage results in mechanical deformation, and this effect is called the converse piezoelectric effect. Sensors and transducers are based on the principle of the direct piezo effect, and actuators operate under the principle of the converse piezo effect.

Direct piezoelectric effect generated across a material can be expressed by the following equation,

$$D = d \times T + \varepsilon \times E, \tag{1}$$

Here, the electric charge density displacement is represented by D, T represents the applied mechanical stress, ε represents the material permittivity, the piezoelectric coefficient (piezoelectric charge constant) is represented by d, and the electric field is represented by E. A higher voltage output can be generated for a material with higher d value for the same amount of mechanical deformation. This value clearly indicates the piezo activity of the material. The piezoelectric charge constant d is defined as the polarization produced for unit mechanical stress applied on the material. This piezoelectric charge constant represents a third rank tensor where it couples between a second rank tensor or vector for stress and a first rank tensor for generated electric potential. Piezoelectric coefficient(d_{ij}) is an anisotropic physical quantity and thus in general it relates input parameters (applied mechanical stress) to output parameters (direction of polarization or electric displacement) associated with piezoelectricity using double subscript. Piezoelectric charge coefficient is a third rank tensor that can be expressed as 3×6 matrix that correlates charge displaced unit area associated with an applied stress according to the relation,

$$D_i = d_{ij} T_j$$

where d_{ij} represents piezoelectric charge coefficient (C//N), D_i represents dielectric displacement (C/m^2), with i denoting the direction of charge motion, and T is the applied stress, with j denoting the direction of applied stress. Thus, d_{33} relates the ratio of charge motion along the third axis (z) to the stress applied along the third axis (z), assuming the electrodes shorted and no other stress is present. Stress represents the applied force acting over the surface area of a material. In other words, we can say that d_{33} means induced polarization along the z-axis per unit stress applied along the z-axis. Here, subscripts 1, 2, and 3 are used for x, y, and z directions, and shear about these axes is represented by 4, 5, and 6. In the case of d_{33}, the directions of polarization and applied force are parallel to each other. The d_{33} value of a material clearly indicates the relationship between crystallization and piezoelectricity.[13,14]

Materials generating a piezo effect that can be easily electrospun into nanofibers mainly include polymers. Polymers that exhibit a piezo effect include natural and synthetic types. Some of the natural organic materials that exhibit a piezo effect include gelatin (d_{33} = 20 pC/N), silk (d_{33} = 38 pC/N), and PLLA (d_{33} = 27 pC/N). Poly(L-lactide) (PLLA) is a piezoelectric polymer with adequate piezoresponse obtained by the ring opening polymerization of an L-lactide monomer. In addition to these, cellulose and chitin also have appreciable piezo activity with less mechanical stability.[15] Some of the synthetic semicrystalline polymers that exhibit piezoelectric properties mainly include polyvinylidene fluoride (PVDF; d_{33} = 20–40 pC/N) and its copolymers trifluoethylene, nylon 66, and poly ureas.[16] A variety of amorphous polymers also exhibit piezoelectric behavior and this category includes polyvinyl chloride (PVC), polyacrylonitrile (PAN), and polyvinyl acetate (PVAc). The main attractive properties that promote these polymers for piezoelectric applications include their high impact resistance, low acoustic and mechanical impedance, high dielectric breakdown, and operating field strength with low density and elastic stiffness.[17,18]

PVDF [$(C_2H_2F_2)_n$] is a semicrystalline thermoplastic fluoropolymer with long-chain molecules produced by the polymerization of the monomer units vinylidene difluoride (CH_2=CF_2). It is a highly stable non-reactive polymer with around 50–60% crystallinity.[19] PVDF typically exists in five crystalline phases, namely α, β, Υ, δ, and ε, due to its polymorphic nature. Here, α, β, and Υ are the more abundant polymorphic phases, out of which β is the main focus of attraction due to its piezoelectric nature. The β phase is the only phase responsible for the piezoresponse of PVDF polymer. The CH_2 and CF_2 groups are found in different spatial arrangements along the polymer chain, and this results in the generation of several fascinating properties of PVDF. PVDF includes around 3 wt.% of hydrogen and 59.4 wt.% of fluorine, and this fluorine content greatly affects the chemical and electrical properties of PVDF. The presence of electronegative fluorine and electropositive hydrogen results in the generation of dipole moment inside the molecular units of PVDF. An orthorhombic crystallographic system with all-trans or TTTT molecular conformation is exhibited by the β polymorph, but α polymorph exhibited a monoclinic crystallographic system with a TGTG′ molecular conformation. A T3GT3G molecular conformation with an orthorhombic crystallographic system is shown by Υ polymorph. The polar and antipolar analogue of the α phase is represented by δ and ε phases.

Journal : Large 11664 | Article No : 11097 | Pages : 18 | MS Code : 11097 | Dispatch : 29-4-2024

The all-trans TTTT planar zigzag molecular conformation of the β phase results in the generation of a non-zero net dipole moment, and the C–F dipoles and C–C chain backbone are arranged in such a way that they cancel each other out. The molecular chain arrangement of the PVDF polymer and the original image of an electrospun PVDF nanomembrane are shown in Fig. 2.[20,21]

The piezoelectric nature of the PVDF nanofiber generates a piezoelectric response, making it suitable for energy harvesting.[22–24] The process of turning wasted or "ambient" energy into useable energy for everyday activities is known as energy harvesting. Although generated power is low for many electrical appliances, it is useful for low-power electronic devices.[25–28] Energy harvesting has various applications such as noise barriers that harness ambient acoustic energy, kinetic energy generators that harness the energy of mild vibrations from common appliances such as ovens and washing machines, and other related uses.[28,29] The PVDF nanofiber is a fantastic material for this application because of its qualities. Of all the piezoelectric polymers, it is lead-free, flexible, and has one of the highest piezoelectric coefficients (d33) of roughly 12 to 35 pC/N.[29,30]

PVDF nanofibers are used in energy harvesting and smart systems as tactile sensors. They detect and measure body signals such as respiratory cycles and heart rate in medical applications. PVDF's fast response time and high sensitivity make it ideal for recording pulses. It is also used in teleoperation, surgeries, and complex systems to detect damage in vital structural parts.[31–37] PVDF sensors can detect damage or cracks in components by measuring strain changes. In addition, their self-excitation property makes them very cost effective for many applications. High sensitivity allows them to accurately detect contact force and tactile "smoothness" of materials, similar to the tactile sense of fingers.[38] PVDF sensors are used for flow velocity measurements in medical research, particularly in sleep apnea. The force of gas on the nanofiber depends on airflow velocity, similar to pneumotachographs. However, more research is needed on the performance of electrospun PVDF nanofibers and the combination of optical and electronic characterizations.[39–45]

Therefore, this work presents a detailed parametric study of PVDF nanofiber membranes, fabricated at different needle-to-collector distances and consequently different applied electric fields. The generated nanofibers are tested through piezoelectricity measurements to detect the optimized electrospinning process parameters for the best piezoelectric performance. In addition, the impact of varied processing parameters is investigated with respect to the surface morphology of the formed PVDF structures, whether in thin film or nanofiber mat form, while also assessing their optical properties and piezoelectric response. To identify the most effective nanomembrane from the piezoelectric perspective, both voltage and power density measurements are performed under different mechanical excitations. In addition, the morphological characterization of the generated samples is analyzed using scanning electron microscopy (SEM) images, while the chemical composition and beta sheet formation are analyzed via Fourier transform infrared (FTIR) spectroscopy. As part of application-based studies, this study applies perturbations in the form of variable momentum and airflow rates to the sample with the best piezoelectric response. These findings will be useful in the application of energy harvesting or airflow sensing to detect gas leakages in complex systems or for generating electricity using wind.

Experimental Work

Materials

Polyvinylidene difluoride (PVDF; Sigma Aldrich) and Kynar® (Arkema , King of Prussia, PA, USA) were the main nanofiber membranes used in the present study. The solvent used for the preparation of PVDF solution was dimethyl formamide (DMF) (98%, Sigma Aldrich, Taufkirchen, Germany). To prepare the solution, 10 g PVDF powder

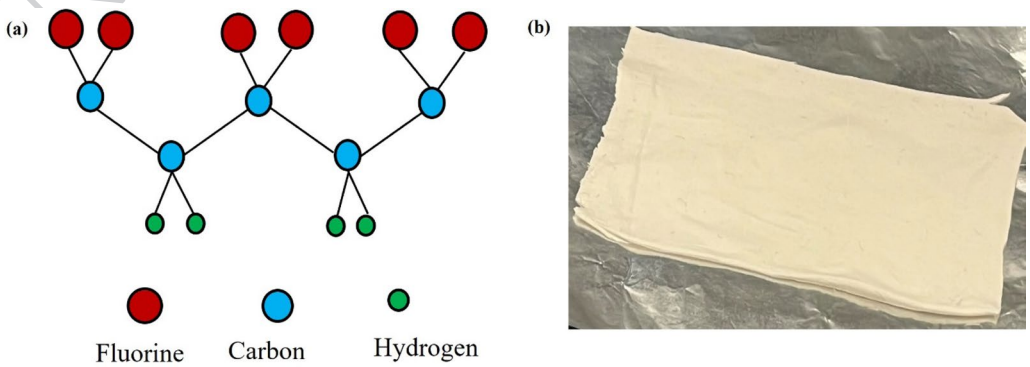

Fig. 2 (a) PVDF chain configuration, (b) A sample of PVDF electrospun nanofiber membrane on an aluminum foil sheet.

Journal : Large 11664 | Article No : 11097 | Pages : 18 | MS Code : 11097 | Dispatch : 29-4-2024

was dissolved in 10 ml DMF and left on a magnetic stirrer overnight to achieve a homogeneous solution of PVDF 10 wt.%. The prepared air bubble-free solution was loaded into a syringe with a needle for electrospinning.

Electrospinning Process

A schematic of the electrospinning setup is shown in Fig. 1. The plastic syringe with a stainless-steel 18-gauge needle was loaded with the required solution and then was fixed onto an injection pump (NE1000-Single Syringe Pump, New Era, Farmingdale, NY, USA) to control the feed rate of the solution during the electrospinning process. The feed rate was set for a flow rate of 2 ml/h, and the distance between the needle and collector was varied within a range from 12 cm to 15 cm to test the effect of needle-to-collector distance on the generated nanofiber membrane. A 30 kV/1.65 mA regulated high-voltage power supply (Divotech Technologies) was used for the application of a constant 22 kV voltage on the metallic needle, and the negative terminal of the power supply was connected to the collector plate, where it was finally grounded. A 15 × 17 cm static copper plate covered with aluminum foil was used as a collector electrode for concentrating the deposition of nanofibers.[46] The generated nanofiber membranes were peeled off carefully from the aluminum foil-covered collector electrode. A total of 10 ml polymer solution was deposited onto the collector electrode at a feed rate of 2 ml/h, and thus a total of 5 h was required for the electrospinning process to fabricate each sample. A set of four PVDF nanomembranes were fabricated by adjusting the needle-to-collector distance from 12 cm to 15 cm in steps of 1 cm. All other process parameters were kept constant throughout the experiment. The high-voltage power supply was adjusted to maintain a voltage of 22 kV throughout the experiment, and the flow rate was fixed for 2 ml/h. The characterization of these nanofiber membranes was done to check the optimum parameters that generated the best nanofiber sample. The nanofiber membranes were cut into an appropriate size of 2 × 2 cm, and these membranes were sandwiched between two aluminum foil sheets from which shielded copper wires were connected. The membrane with aluminum foils sheets was made into a single unit using paper tape. Finally, the sample was fixed horizontally without any air gap onto the base of the custom-made setup for piezo characterization in order to apply a vertical force onto the sample.

Impact of Momentum on PVDF Nanofiber Applications

The fabricated nanofiber membrane displaying the best piezoelectric performance was cut into a piece of 2 × 2 cm, and the sample was sandwiched between two aluminum foil electrodes connected to insulated copper wires and then integrated inside two setups to detect both shutter velocity and airflow speed. The best fabricated nanofiber was electrospun at a needle-to-collector distance of 15 cm at an applied voltage of 22 kV with a flow rate of 2 ml/h.

As shown in Fig. 3, the experimental setup for inspecting the impact of momentum included a frictionless air track with a freely moving cart controlled by a magnet at the starting position, where additional mass could also be added. The sample was positioned vertically in the path of the cart with a head radius 1 cm. The cart hit the nanofiber membrane in a horizontal direction at different applied velocities, and the impacts resulted in the generation of piezoelectric voltage. Piezoelectric voltage that developed in response to the applied velocities were recorded via an oscilloscope by connecting the insulated shielded wires to both aluminum foils. The experiment was performed three times. First, the impact of different applied velocities ranging from 0.1 m/s to 0.5 m/s was investigated on the first sample, after which the same procedure was repeated by changing the first sample with a second sample. Piezoelectric voltage generated for the second sample was also recorded. Finally, the two sample pieces were attached together by removing the insulated wires on one side of the samples and then attaching them together using the conducting aluminum foil sheets such that the double-layer sample acted as a single piece. The piezoelectric voltage generation for this third sample, which was the combination (series-like combination) of the two sample pieces, was studied. The arrangement of the single-layer and double-layer nanomats between the conducting electrodes is represented in detail in Fig. 3. Two single layers are attached in such a way that the bottom portion of the second layer is directly attached to the top portion of the first layer without any air gap, and thus a series connection is maintained between them.

Airflow Sensing Studies of the Fabricated Nanofiber Applications

The setup used to create the airflow, as shown in Fig. 4, consists of an electric air duster with an attached nozzle (1 cm radius), which was pointed at the center of the PVDF sandwiched unit. In order to change the speed of the airflow from the air duster, the distance was varied for each speed, which was measured using a velocity meter placed on a table and a ruler to measure the distance between the air duster's nozzle tip and the fan blade of the velocity meter. For each airflow speed value, the air duster was held at the corresponding height and pointed at the center of the sample. The sample was exposed to the airflow for

Journal : Large 11664 | Article No : 11097 | Pages : 18 | MS Code : 11097 | Dispatch : 29-4-2024

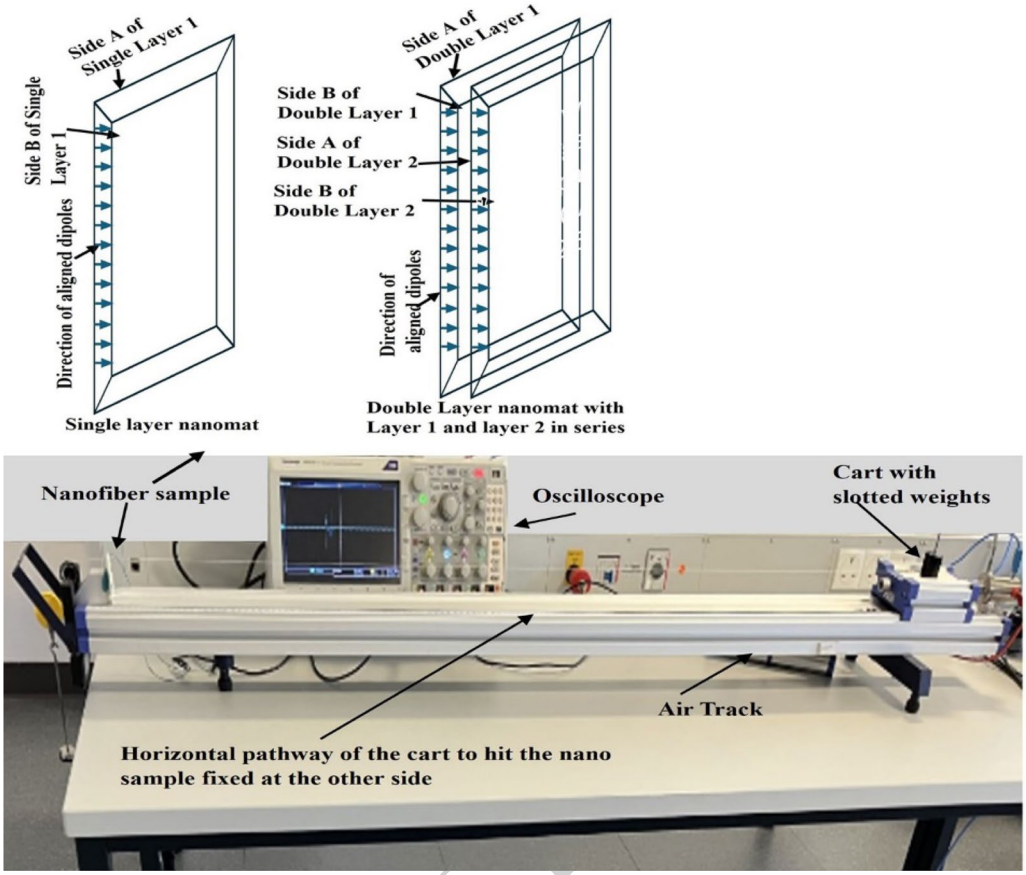

Fig. 3 Experimental setup used for the momentum and velocity response analysis.

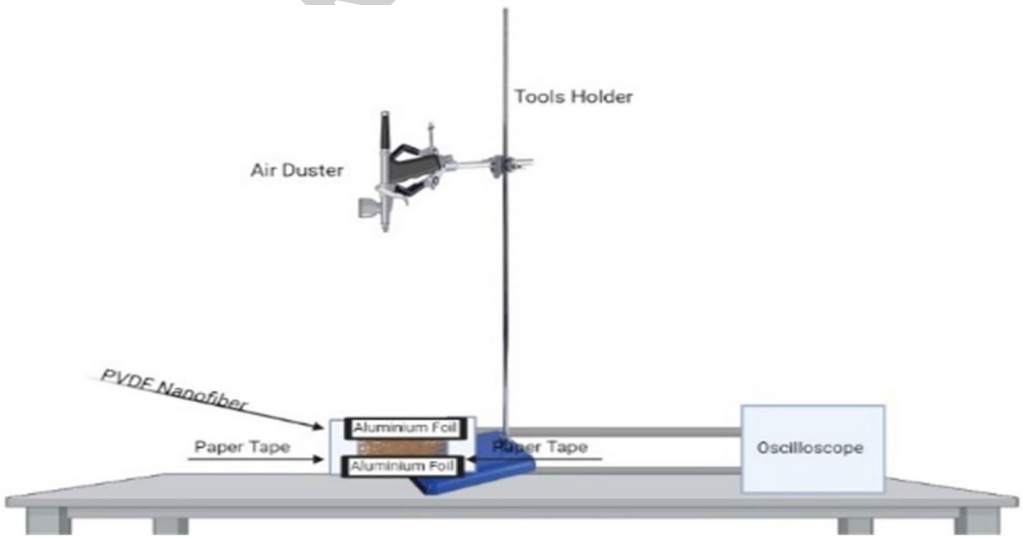

Fig. 4 Experimental setup used for PVDF airflow sensing-based analysis.

| Journal : Large 11664 | Article No : 11097 | Pages : 18 | MS Code : 11097 | Dispatch : 29-4-2024 |

1 s, and the average was calculated by taking six different peak-to-peak voltage readings from the given signal on the oscilloscope.

Characterization of the Fabricated Nanofiber Membrane

Optical Characterization

The optical characterization of the set of four samples fabricated at different needle-to-collector distances was performed using a UV-Vis spectrophotometer (Shimadzu UV-2600). The optical characterization includes the generated nanofiber absorbance and transmittance analysis. Here, the sample to be analyzed was illuminated by a light source in the wavelength range from 190 nm to 900 nm. The experimental setup mainly includes a light source, a monochromator or a prism to separate wavelengths, a sample holder, and a detector. Transmittance and absorbance measurements were based on the comparison of light intensity before and after passing through the sample to be tested. Transmittance can be defined as the ratio I/I_o where I represents the intensity of the light after passing through the sample and I_o represents the full intensity of light before passing through the sample. The absorbance is the amount of light absorbed out of the incident light by the sample. The optical activity of the generated sample indicates the potential of these membranes in the field of light-based or transparency-based applications such as touch panels and transparent wearable sensors.

Chemical Characterization

FTIR spectroscopy was used to analyze the response of these nanofibers towards the piezo activity based on the beta sheet content. The molecular fingerprint of the sample can be easily analyzed using FTIR spectra based on the functional groups present and the interactions between them. The transmittance spectra of the PVDF nanofibers were generated using a PerkinElmer FTIR spectrometer at a scanning resolution of 5 cm^{-1} around a range of 4100–400 cm^{-1}. Each sample was scanned about 120 times while generating the transmittance spectra. Determining the chemical structure of a sample is mainly based on the molecular vibrations. Stretching and bending are the two types of molecular vibrations involved in IR spectroscopy. The stretching mode changes the bond length, resulting in either symmetric or asymmetric mode, whereas the bending mode always changes the bond angle. Whenever the frequency of a specific bond vibration becomes exactly equal to the frequency of the applied IR radiation, the radiation will be completely absorbed by the sample content, generating a plot of transmittance.

Morphological Characterization

A nanofiber sample measuring 1 × 1 cm was analyzed using a scanning electron microscope (JEOL JSM-7610FPlus FESEM, Jaipur, India) to study the surface and morphology of the generated nanofiber mat. The nanofiber size distribution on the fabricated membrane was studied and measured using ImageJ software.

Piezoelectric Characterization

Piezoelectric characterization associated with the fabricated nanofibers was performed using an applied perturbation in the form of falling masses and applied forces, and the corresponding generated voltage was measured directly using an oscilloscope. The generated voltages were measured across different load resistance.

Voltage Characterization

The piezoelectric characterization of nanofibers includes different applied force and frequency measurements, as presented in Fig. 5. Different compressive loads/forces from 0.5 N to 3 N in steps of 0.5 N were applied onto the nanofiber sample at a single frequency of 1 Hz, and the corresponding generated voltage was measured. Frequency measurements were performed by varying the frequency between 0.25 Hz up to 10 Hz at a specific applied force of 2 N and measuring the corresponding generated piezoelectric voltages.

In addition, piezoelectric characterization based on impulse loading at a height of 2 cm was also performed. Impulse loading shows the effect of masses falling onto the sample, where the mass was varied from 50 g to 250 g and the generated output voltage was measured.

Power Density Characterization

As shown in Fig. 6, the piezoelectric performance of each sample based on different applied load resistance across the positive and negative electrode plates was studied. Different load resistance was applied across the electrodes as part of the characterization. Here, the oscilloscope probe was connected across the positive and negative electrode plates through the load resistance. Finally, the power output obtained for each sample was calculated over the area of impact to obtain power density and plotted against the

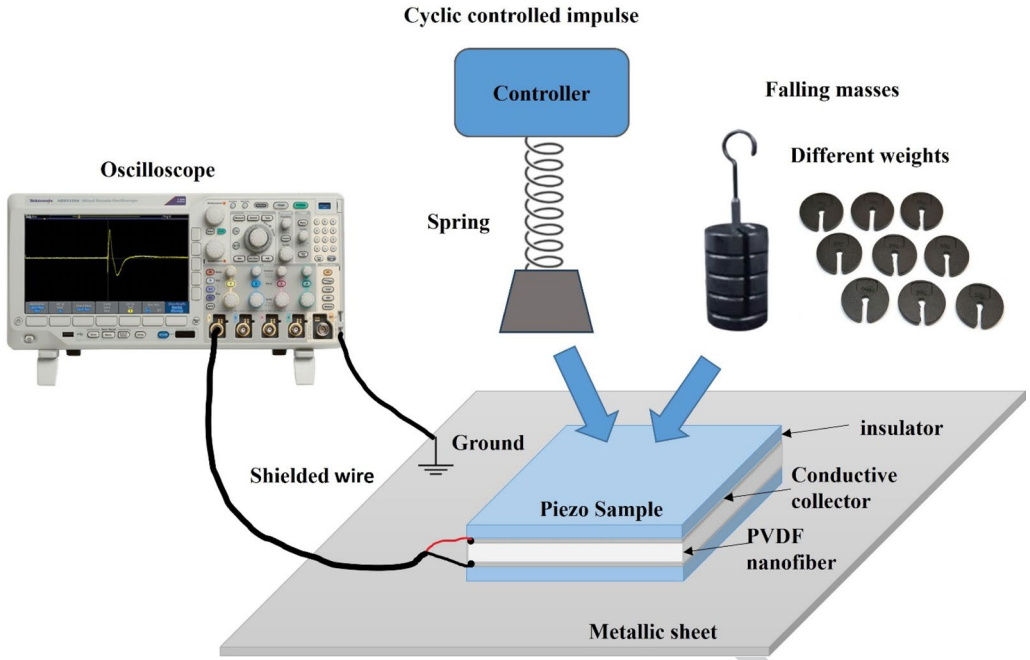

Fig. 5 Experimental setup used for the piezo characterization of the PVDF electrospun mat.

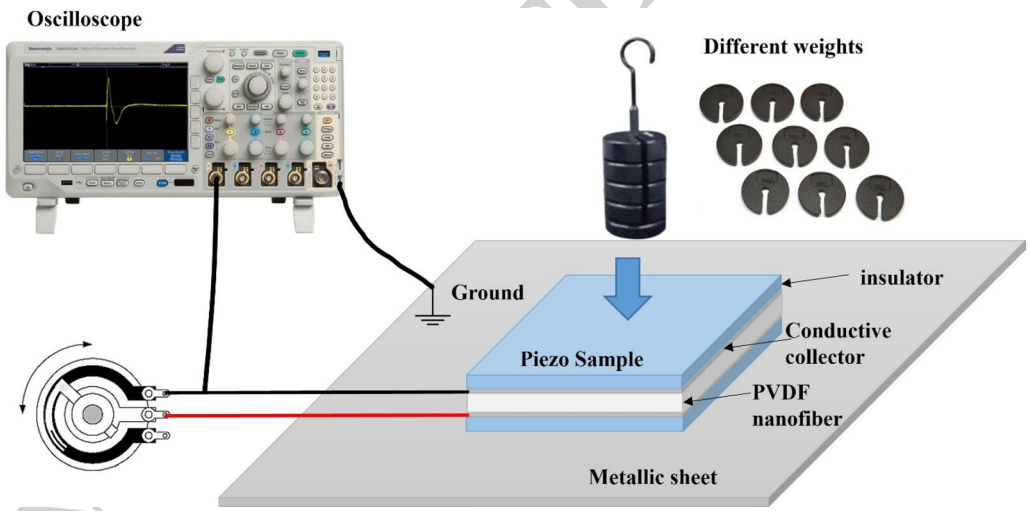

Fig. 6 Experimental setup used for the power density measurements of the PVDF electrospun mat.

corresponding load resistance. The area of contact in the present study is circular with an effective radius of around 1.4 cm. The power density plots give us an indication of the efficiency of the fabricated nanomembrane towards some resistive loads in terms of piezo activity.[47]

Results and Discussion

Optical Characterization

Optical characterization of the set of samples was performed using UV-Vis spectrophotometry, recording absorbance and transmittance data. The absorbance spectra of the corresponding samples are shown in Fig. 7. The nanofiber membrane showed clear optical absorption in the region from

Journal : Large 11664 | Article No : 11097 | Pages : 18 | MS Code : 11097 | Dispatch : 29-4-2024

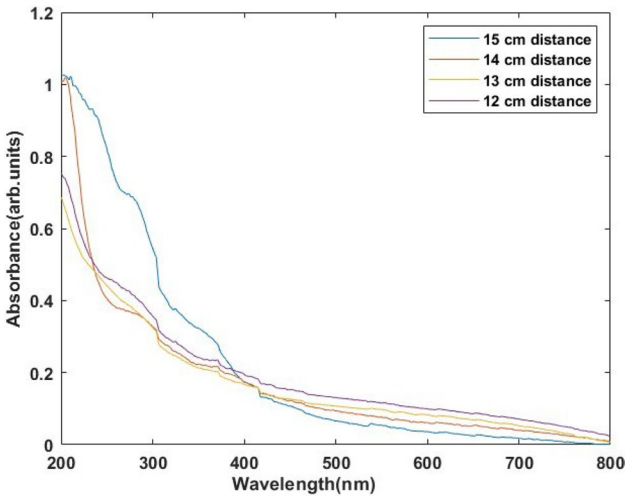

Fig. 7 Absorbance spectra of pure PVDF nanofiber samples.

200 nm to 400 nm, which clearly shows the absorption peak of the PVDF polymer. Absorbance spectra of the samples clearly indicates the optimum performance of the nanofiber membrane fabricated at a needle-to-collector distance of 15 cm, where maximum absorption intensity is obtained. We can conclude from the absorbance curve that the PVDF content is greater in the nanofiber membrane electrospun at distances of 15 and 14 cm, with good nanofiber content, whereas the remaining two samples displayed lower absorption intensity. In the visible range, the mat electrospun at 12 cm exhibited scattering effects near the baseline, thereby generating good absorption in the visible region compared to other electrospun mats.[48]

Transmittance analysis of the samples is shown in Fig. 8. Maximum transmittance is found for the nanofiber samples fabricated at a needle-to-collector distance of 12 cm, which exhibited a film-like behavior. This clearly confirms the transparency of this sample. Nanofiber membranes electrospun at a distance of 15 cm showed the lowest transparency, with good absorbance. Nanofiber membranes developed at distances of 14 and 13 cm also showed good absorbance and low transparency. The most transparent samples exhibited film-like behavior, with less piezo activity, as will be verified later. Optical characterization of these samples revealed the absorbance and transmittance rate for each sample. The nanofiber membrane fabricated at a distance of 15 cm consists of a rough surface with numerous pores and solid fibers. This structure creates some opaqueness towards light, resulting in weakly transparent behavior. Here, the pores are interconnected, resulting in the development of dozens of fiber–air interfaces, and in this case, interfacial adherence and packing density has to be considered, which ultimately promotes the hazy appearance towards light. When considering the internal structure, we should take into account the air present inside the nanofiber which promotes the scattering of light to a great extent, further reducing the transmittance. All these effects are identified in the presence of fiber-like structures. The film electrospun at a distance of 12 cm consists of fewer pores and fiber-like structures, resulting in appreciable transparency that allows light to pass through. Thus, transparency is found to decrease with an increase in the feeder-to-collector distance from 12 cm to 15 cm, where the fiber-like structure formation originates above 12 cm, and complete development of fibers occurs at 15 cm.[48,49]

In addition, the film cast at a distance of 12 cm consists of fewer pores and the smallest number of fiber-like structures, allowing the effective transmittance of light. Here, the majority of chains are formed as film without successful cross-linking and interconnected networks, promoting higher transmittance through it. The transparency of a polymer-based electrospun mat mainly depends on its crystallinity. Materials with higher crystallinity exhibit less transmittance. This is clearly evident from the FTIR spectra calculation, which shows that the 12 cm-based mat exhibits the lowest beta sheet content, indicating lower crystallinity and thereby showing excellent transparency.[48]

Chemical Characterization

The crystal phases of the pure PVDF nanofiber membrane are clearly projected in the IR transmittance spectra shown in Fig. 9. The most prominent bands related to the crystal phase of PVDF are observed in the wave number range from 700 cm^{-1} to 1500 cm^{-1}.[50] Among these, the transmittance peaks observed at 762 cm^{-1}, 796 cm^{-1}, 875 cm^{-1}, 976 cm^{-1}, 1210 cm^{-1}, and 1383 cm^{-1} correspond to the α phase, and peaks at 840 cm^{-1}, 880 cm^{-1}, 1175 cm^{-1}, and 1275 cm^{-1} are clearly associated with the β phase. The relative fraction of beta phase content can be calculated from the intensity of absorbance bands at 762 cm^{-1} and 840 cm^{-1} using the Beer–Lambert law as shown in Eq. 2 given below:[51]

$$f(\beta) = \frac{A_\beta}{1.26A_\alpha + A_\beta} \tag{2}$$

where A_β represents the absorbance value at 840 cm^{-1} and A_α represents the absorbance value at 762 cm^{-1}.

The absorbance peak corresponding to the α crystalline phase at 762 cm^{-1} is due to the skeletal bending vibration mode C(H)–C(F)–C(H) and CF_2 bending mode. Similarly, the absorbance peak at 840 cm^{-1} due to the polar beta phase represents a rocking vibrational band due to CH_2. Based on Eq. 2, the beta phase content associated with each nanomat fabricated at different needle-to-collector distances is calculated and given in Table I.[52]

Journal : Large 11664 | Article No : 11097 | Pages : 18 | MS Code : 11097 | Dispatch : 29-4-2024

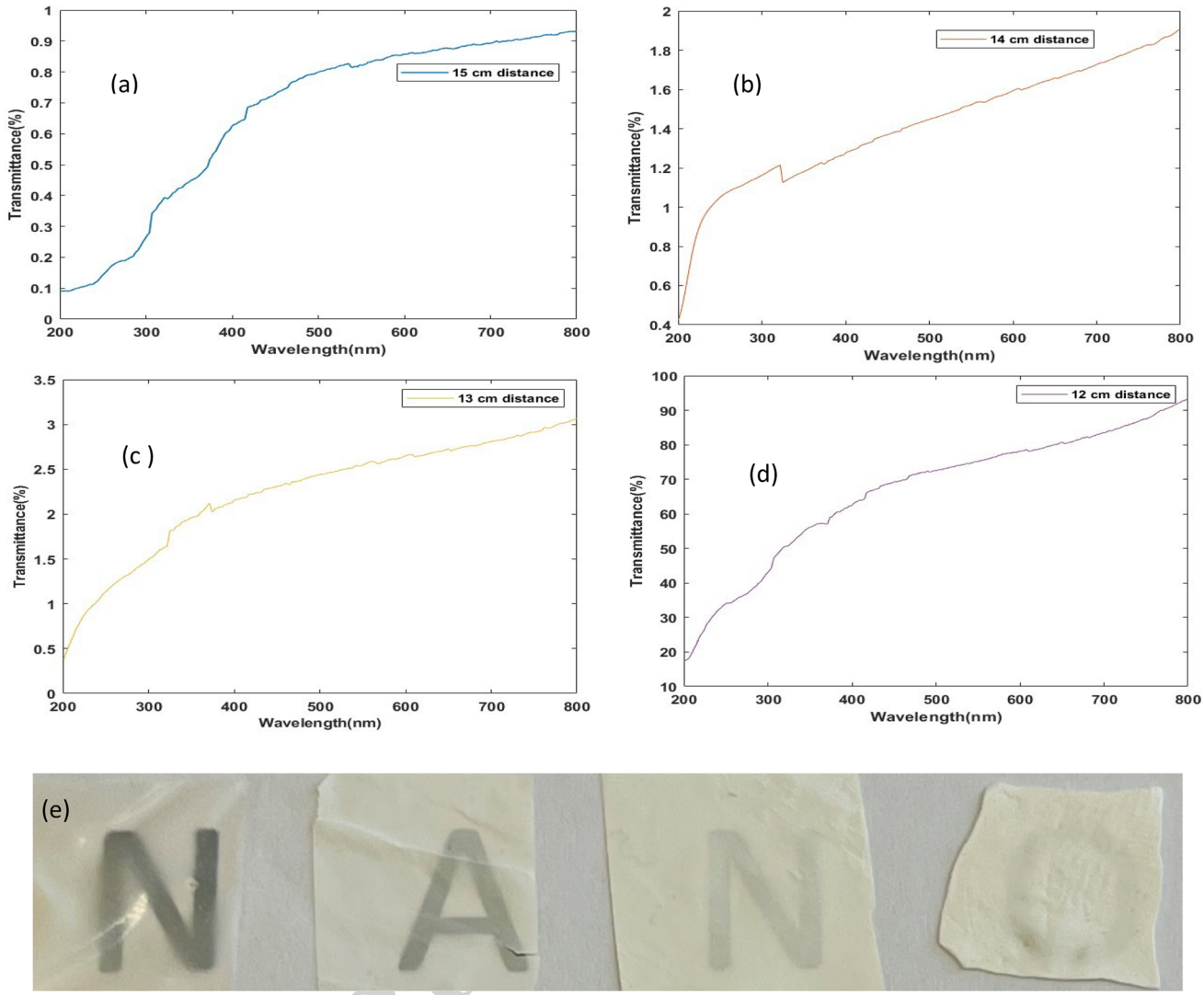

Fig. 8 (a–d) Transmittance of electrospun samples at different feeder-to-collector distances. (e) The letters N, A, N, O correspond to the samples fabricated at feeder-to-collector distances of 12, 13, 14, and 15 cm, respectively, from left to right.

The beta phase calculation revealed that the electroactive polar phase is maximum for the nanomat fabricated at a needle-to-collector distance of 15 cm and is found to be decreasing while reducing the distance from 15 cm down to 12 cm. The beta phase content is due to the CH_2–CF_2 dipole generation inside the PVDF nanomaterial, resulting in an excellent piezoresponse.

Morphological Characterization

Figure 10 shows the SEM images of the electrospun mats generated at different feeder-to-collector distances of 12 cm, 13 cm, 14 cm, and 15 cm. The electrospun mat fabricated at a distance of 12 cm exhibited a thin film-like behavior, as shown in Fig. 10a. Upon increasing the distance from 12 cm to 13 cm, the electrospun mat shows a tendency for fiber generation from the cast film with an uneven surface, as shown in Fig. 10b. Further increasing the distance from 13 cm to 14 cm leads to the formation of more fiber-like structures, as shown in Fig. 10c. In general, the tendency to form fibers is improved by increasing the feeder-to-collector distance. Finally, after reaching a distance of 15 cm, ultrafine nanofibers are clearly observed in the SEM image, represented by Fig. 10d. Thus, a feeder-to-collector distance of 15 cm resulted in the production of the best nanofibers based on the morphological analysis. The increased distance between the needle and collector provides an extended solvent evaporation time during solution travel and deposition. Along the pathway from the needle tip to the collector electrode, successful fiber generation is possible only if an optimum journey time is obtained. Solvent evaporation time should be optimum for obtaining nanofibers with good morphology.

Journal : Large 11664 | Article No : 11097 | Pages : 18 | MS Code : 11097 | Dispatch : 29-4-2024

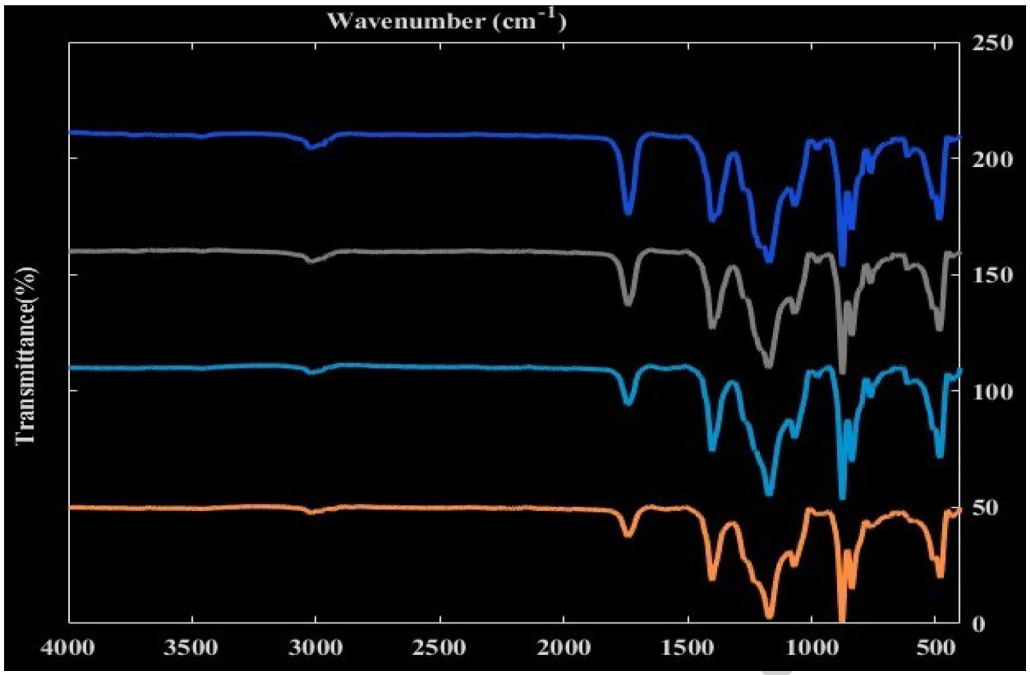

Fig. 9 The FTIR spectra of the generated nanomats.

Table I Calculated beta phase content percentage of the electrospun PVDF nanomats

Sample	$A(\alpha)$	$A(\beta)$	$f(\beta)$
15 cm	0.039976	0.187	0.7877
14 cm	0.06004	0.2237	0.7477
13 cm	0.065	0.196	0.705
12 cm	0.0785	0.2277	0.697

The numbers in the sample column refer to the distance between the feeder and collector in the electrospinning setup

However, increasing the distance above a certain limit reduces the electric force of attraction, negatively affecting the fiber production. This clearly shows that a feeder-to-collector distance of 15 cm is optimum, providing enough time for the deposition of charged fluid onto the collector in the form of fine ultrathin nanofibers after the successful removal of the volatile solvent. In other cases, decreasing the distance between the needle and collector affects the fiber generation due to the lack of successful evaporation of the solvent from the solution for fine solid nanofiber deposition. The SEM image of the nanomembrane produced at a feeder-to-collector distance of 15 cm was analyzed using ImageJ software, and the diameter of the randomly distributed nanofibers was measured. The average diameter of the generated nanofibers was measured to be around 112.8 nm, and the corresponding fiber diameter distribution is shown in Fig. 11.[53]

Piezoelectric Characterization

Voltage Characterization

A variable force or compression load from 0.5 N to 3 N was applied to the nanofiber sample using a spring-based motor arrangement, which is a custom-made setup that allows different vertical forces or frequencies to be applied onto the surface of the sample. The response of a set of four nanofibers fabricated via electrospinning at needle-to-collector distances of 12 cm, 13 cm, 14 cm, and 15 cm was studied. Optimum piezoresponse to the variable forces was shown by nanofibers at a needle-to-collector distance of 15 cm. Nanofibers fabricated at a needle-to-collector distance of 13 cm also showed good piezoresponse, but it was less than that of the sample prepared at the 15 cm distance. The force–voltage relationship developed on the nanofibers is shown in Fig. 12a. The piezoresponse towards the applied force or compression load showed a positive result, where the piezo voltage increased with increased loads. The piezoresponse of the nanofiber fabricated at a needle-to-collector distance of 15 cm showed a weaker response to lower loads, strengthening for higher loads, compared with other samples. The variation in the AC sinusoidal voltage obtained from each nanomembrane fabricated at different feeder-to-collector distances under a specific applied force of 3 N is shown in Fig. 12b. In general, for all the nanofiber membranes, an increase in voltage is observed with increasing loads. The piezoresponse

Journal : Large 11664 | Article No : 11097 | Pages : 18 | MS Code : 11097 | Dispatch : 29-4-2024

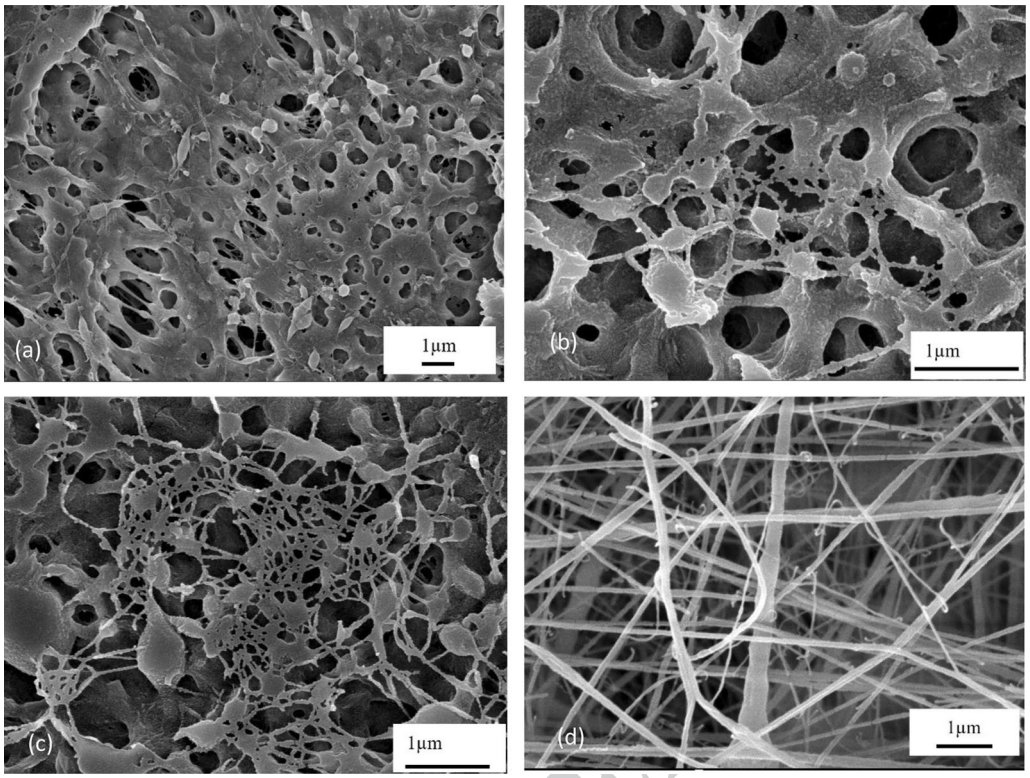

Fig. 10 SEM images of the pure PVDF nanomats fabricated at a feeder-to-collector distance of (a) 12 cm; (b) 13 cm; (c) 14 cm; (d) 15 cm.

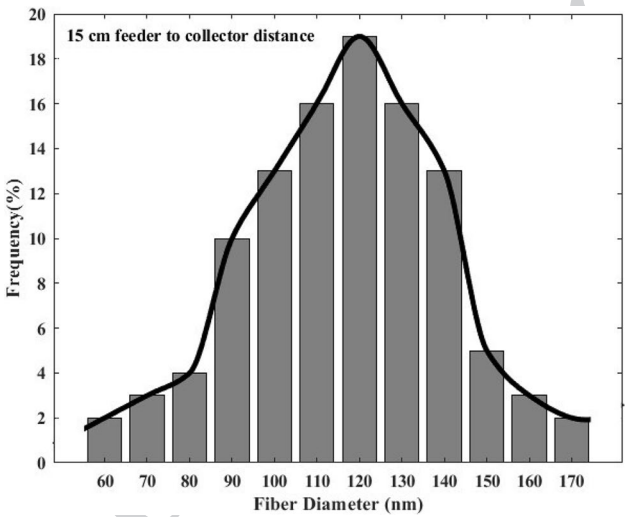

Fig. 11 Electrospun PVDF nanofiber diameter distribution curve.

of the samples to the load is indicated by a sensitivity parameter, which represents the slope of the force–voltage graph. Linear fitting of the experimental data clearly showed a piezo sensitivity of 1.2 V/N for the nanofiber sample fabricated at a needle-to-collector distance of 15 cm. Mats produced at needle-to-collector distances of 12 cm, 13 cm, and 14 cm showed a sensitivity of 0.27 V/N, 1.15 V/N, and 0.9 V/N, respectively. Samples developed at needle-to-collector distances of 15 cm and 13 cm showed the most effective response.

Out of the four electrospun mats, the electrospun nanomat generated at a feeder-to-collector distance of 15 cm exhibited the best piezoresponse. Here, the generation of nanofibers resulted in the formation of a higher density of dipoles upon excitation with applied forces. The distance affects the applied electric field on the PVDF polymeric jet between feeder and collector. This electric field controls the formed piezoelectric properties according to their impact on the alignment of electric dipoles inside the nanofibers. This resulted in the generation of a higher piezoresponse voltage and consequently higher beta sheet content. In the case of the mat electrospun at 14 cm feeder-to-collector distance, the fabrication of nanofiber-like structures are not completely successful, but some fiber generation is confirmed from the SEM image. Thus, lower dipole densities are obtained upon excitation forces compared with mats produced at the 15 cm distance. Their beta sheet contents were also found to be lower than those of the nanomats produced at the 15 cm, resulting in weaker responses. The mat electrospun at 13 cm feeder-to-collector distance resulted in the generation of larger, non-homogeneous beads and fewer fiber-like structures compared to the mat produced at 14 cm. The formation of beads results in the generation of a greater piezoresponse

Journal : Large 11664 | Article No : 11097 | Pages : 18 | MS Code : 11097 | Dispatch : 29-4-2024

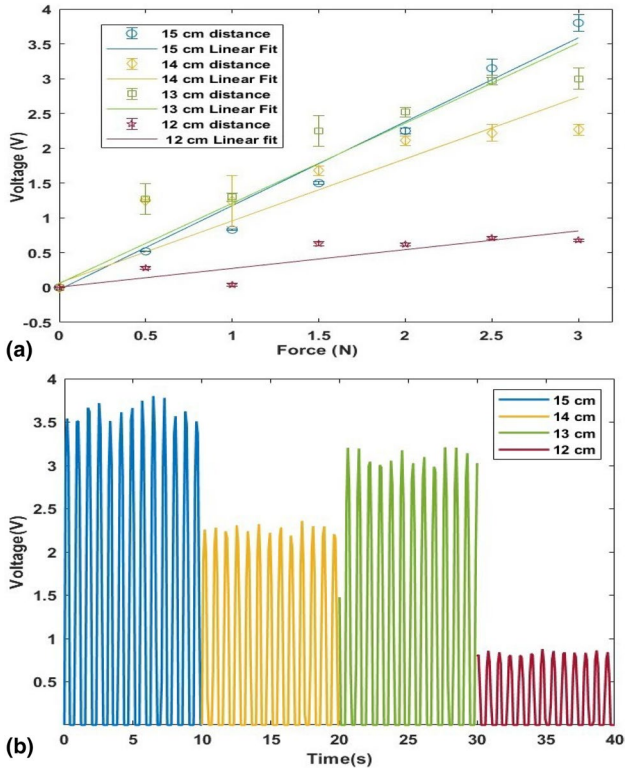

Fig. 12 (a) Applied force versus piezo voltage for pure PVDF nanofiber membrane. (b) An example of AC sinusoidal voltage developed at 3 N force for different feeder-to-collector distances.

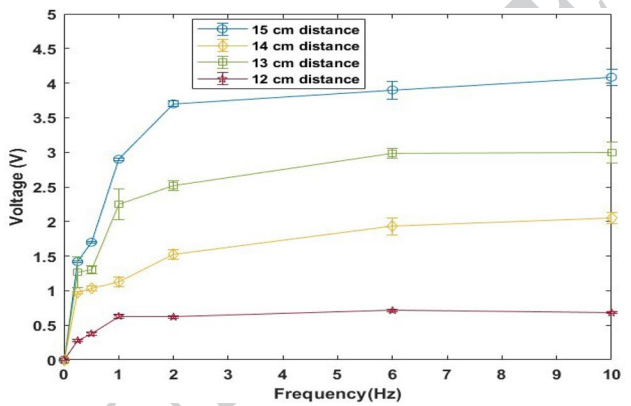

Fig. 13 Applied frequency versus piezoelectric voltage for pure PVDF nanofiber membrane.

than the mat produced at 14 cm, but with a lower beta sheet content due to the presence of a large number of non-homogeneous beads. Finally, the electrospun mat fabricated at a 12 cm distance exhibited thin cast film-like behavior and consequently weak piezoresponse. Thus, we can conclude that more beads were produced as a result of reducing the TCD (tip-to-collector distance) from 15 cm to 13 cm, and a simultaneous departure from a fiber-like structure. Higher piezo voltage for the 13 cm TCD was produced owing to the presence of beads in a significant section of the electrospun mat. Additionally, the beta phase content is significantly reduced by the non-homogeneous distribution of beads, which lowers the crystallinity content. The transmittance of the electrospun mat is drastically improved by a decrease in crystallinity and beta sheet content, which explains why the transparent electrospun mat in this work was created at a lower TCD.[48,54,55]

Effects of needle-to-collector distance on the piezoresponse of nanofiber membranes are analyzed based on cyclic forces. Different cyclic forces of specific frequencies between 0.25 Hz and 10 Hz at a constant force of 2 N are applied on these samples. Frequency-based piezo analysis curves are represented in Fig. 13. The curves clearly indicate a linear response to lower frequencies from 0.5 Hz to 2 Hz and saturation for higher frequencies of 6 Hz and 8 Hz.

Optimum piezo performance based on frequency was also shown by the nanofiber membrane fabricated at a needle-to-collector distance of 15 cm. A needle-to-collector distance of 13 cm showed appreciable behavior, but it was less than that of the sample prepared using the distance of 15 cm. In general, the piezoresponse was found to be the best and most consistent for nanofibers fabricated at a needle-to-collector distance of 15 cm.

The active piezoresponse shown by the nanofiber membrane electrospun at 15 cm compared to that electrospun at 12 cm can be explained in terms of the higher surface-to-volume ratio and porosity of the nanofiber membrane. Piezoelectric materials are commonly non-centrosymmetric materials, and as a result, the application of a vertical force or stress perpendicular to the sample shifts the center of mass of positive and negative ions, creating a net polarization inside the material. Thus, a voltage difference or potential between two surfaces of the PVDF sample is generated via dipole generation throughout the materials by changing its dimensions. The dipoles inside the material usually cancel each other out; however, the dipoles at the surface do not, which produces polarity. When these samples are in the form of one-dimensional nanofibers, their surface-to-volume ratio and porosity increase extensively compared to the electrospun film counterparts. As a result, a higher dipole surface-to-volume ratio is seen in the case of the nanofiber membrane, resulting in the efficient extraction of voltage compared to the electrospun cast film counterpart.[56] The main dipoles inside the PVDF material are CH_2–CF_2, accounting for the development of an electroactive beta phase and higher piezoresponse. In addition, the higher surface-to-volume ratio favors the trapping of electrostatic charges. Consequently, under deformation, trapped charges generate voltage and current. For the case of 13 cm and 14 cm membranes, the fiber formation was only initiated

Journal : Large 11664 | Article No : 11097 | Pages : 18 | MS Code : 11097 | Dispatch : 29-4-2024

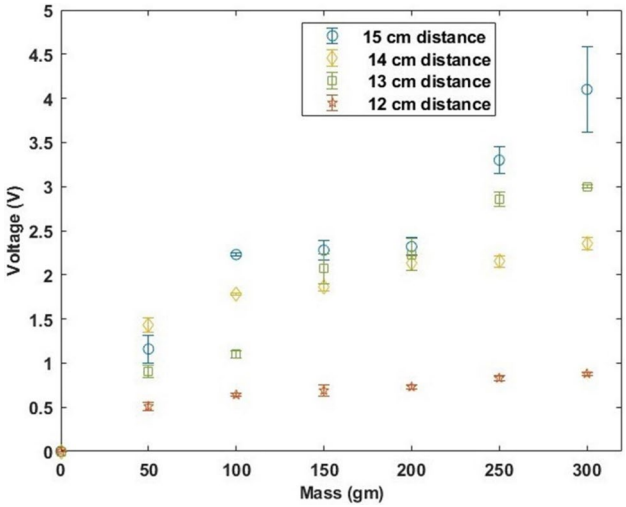

Fig. 14 Applied mass versus piezoelectric voltage for pure PVDF nanofiber membrane

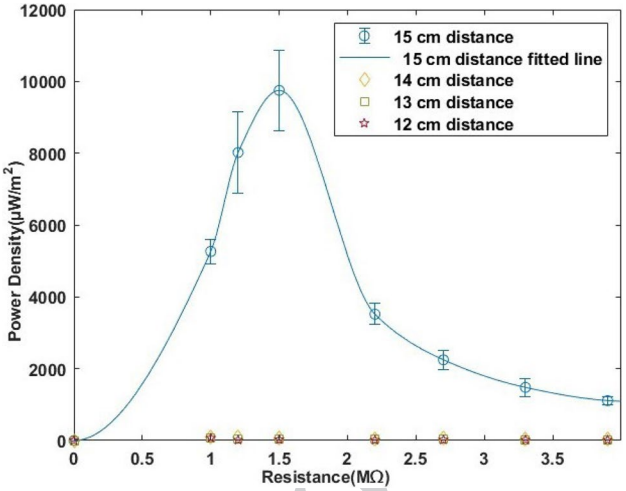

Fig. 15 The plot of power density versus load resistance for the PVDF nanofiber membrane.

and not completely developed, generating less voltage than the 15 cm sample. Thus, the excellent porosity and higher surface-to-volume ratio of nanofiber membranes result in the highest piezoresponse, with significant electroactive beta phase content in the case of the 15 cm nanofiber membrane.[57]

Impulse load testing shows the effect of falling masses, and the associated impact results in the generation of voltage. The associated voltage curves are shown in Fig. 14, which clearly show the increase in voltage generation with increased falling masses. Impulse load piezo analysis was performed for the set of samples, showing an appreciable response for the 13 cm nanofiber samples, and maximum voltage generation was found for the 15 cm nanofibers. Thus, a positive correlation exists between applied mass and generated voltage for all the samples.[52] A maximum potential of 3.2 V is obtained by the application of 3 N force, and a generation of around 4.5 V is observed through impulse loading during the application of a mass of 300 g from a height of 2 cm. Cyclic force or frequency-based mechanical stress produced a maximum force of 3.2 V at a frequency of 10 Hz.

Power Density Characterization

The generated piezo voltage is dependent on the load resistance connected externally across the electrodes, which is used for the estimation of power. Power density calculations for the generated samples exhibited random behavior. This was exhibited by random power increases for certain resistance loads, followed by decreasing power density output with increasing load resistance, and then again, an increase in the power density output was observed for further increases in the applied resistance loads. But this fluctuating behavior was not present in the case of the nanofiber membrane fabricated at a needle-to-collector distance of 15 cm, where a prominent Lorentzian curve was obtained for the power density plot. Here, maximum power density was obtained for a resistance load of 1.5 MΩ, followed by a gradual decrease with an increase in the resistance load from 2.2 MΩ, 2.7 MΩ, 3.3 MΩ, and 3.7 MΩ, and the corresponding plot is shown in Fig. 15. A maximum power density of 9.7 mW/m^2 was obtained for a potential of 3 V in the case of the PVDF nanofiber mat fabricated at a distance of 15 cm.[58]

Impact of Momentum on the Nanofiber Membrane

One of the primary sources of mechanical energy present in the majority of engineering application systems is mechanical shock. By altering the object's momentum and the speed at which it strikes the sample, the reaction of the electrospun nanomat to mechanical shocks is examined. The findings reveal a favorable reaction to mechanical shocks, demonstrating the potential of these nanomats for energy harvesting applications involving mechanical shocks. Therefore, by altering the momentum's effect on the nanomats, this paper's concept is to use these sensitive nanofiber mats as a piezo or vibration energy harvester to extract electrical energy from mechanical shocks. The effect of applied mechanical shocks on the nanomats is varied by changing the velocity with which the frictionless cart is horizontally hitting the sample. The momentum of the cart is represented as the product of its mass and velocity. First, the impact of different applied velocities from 0.1 m/s to 0.5 m/s on the first sample piece was studied, after which the same procedure was repeated by changing the first sample with the second sample. Even though the sample pieces were taken from the same nanofiber membrane sheet, the piezoresponse

Journal : Large 11664 | Article No : 11097 | Pages : 18 | MS Code : 11097 | Dispatch : 29-4-2024

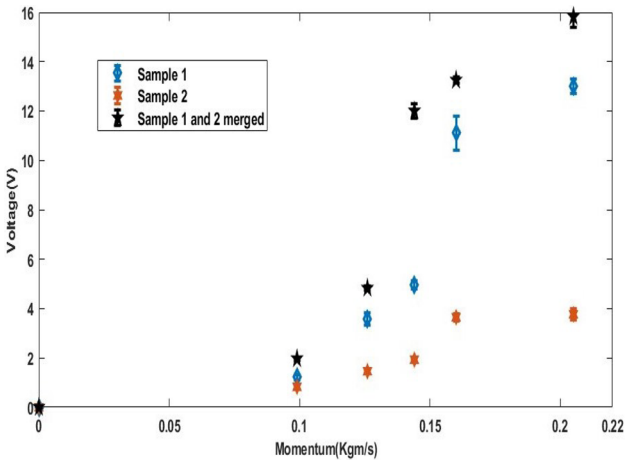

Fig. 16 Piezo voltage analysis based on the impact of momentum in pure PVDF nanofiber membrane.

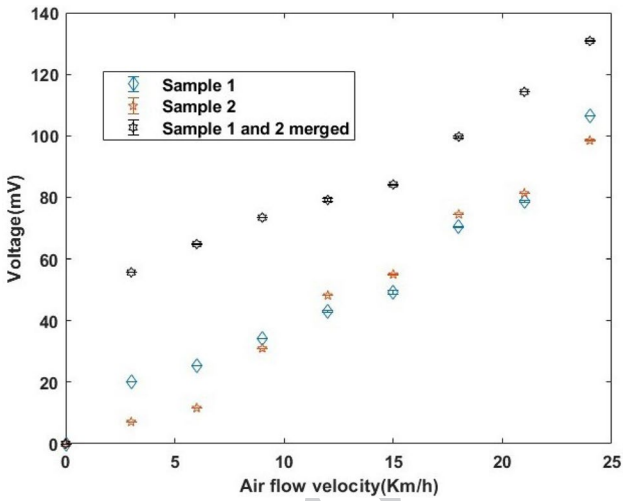

Fig. 17 Voltage versus airflow velocity for pure PVDF nanofiber membrane.

shown for the same velocity values were different. The first piece, labeled sample 1, showed a good piezoresponse in the range 1.8–12.5 V compared to the second sample. The second sample generated less voltage in the range of 0.5–3.8 V. The piezoelectric voltage output generated in each case is shown in Fig. 16. The combined sample, labeled as sample 3, showed the highest voltage output, which was almost the sum of the voltage generated for samples 1 and 2. For both single- and double-layer formations, the mechanism of similarly aligned diploes within the two layers produced a similar impact to series connections of the two layers, which led to incrementally higher generated voltage compared to the single-layer case, as clearly shown in Fig. 3. The series combination of the two pieces in effect showed the double-layer effect, which clearly enhanced the performance of the energy harvester, generating a voltage in the range of 2–16 V. This clearly indicates that the addition of different layers of PVDF nanofiber membrane can enhance the piezoresponse to a great extent, which is promising for several applications. The addition of two layers of PVDF nanofiber membrane greatly enhanced the durability of the sample. Thus, the double-layer sample not only improved the piezoresponse, but also greatly enhanced the mechanical stability.

Thus, the impact of momentum on these samples is studied by varying the applied velocity, and the efficiency of the fabricated nanomats in the field of energy harvesting from mechanical shocks is clearly proved in the present study.

Airflow Sensing Studies of the PVDF Nanofiber Membrane

For each airflow speed value, the air duster was held at the corresponding height and pointed at the center of the sample. The sample was exposed to the airflow for 1 s and the average was calculated by taking six different peak-to-peak voltage readings from the given signal on the oscilloscope. Due to external factors, constant noise was shown on the oscilloscope (ranging from 20 mV to 40 mV). Before each measurement, the noise was first recorded and then subtracted from the reading after the measurement. For the double-layer PVDF sample, the original single-layer sample was paired with another sample, which was prepared in the same manner and tested for its piezoresponse. Each sample had a piece of aluminum foil on one side (the outer side) and one shared piece of aluminum foil in between. The samples were then framed with paper tape and had one wire on either side, making it a series circuit. Due to the experimental setup, as the distance between the electric duster's nozzle and the PVDF sample increased, the air was more dispersed and less directed towards the sample, resulting in a lack of smoothness. This increase is seen in the graphs in Fig. 17, which show an obvious relationship in the graphs regardless. When the two samples were put together to create the double-layer sample, there was an increase in the output voltage of the PVDF sample; however, it was not exactly equal to the sum of the voltages of the two samples. This is because the layer of PVDF that experiences direct impact from the electric duster's airflow absorbs some of the force, meaning that less of it impacts the second layer.

The detailed results regarding the piezo voltage generated from the samples are listed in Table II. The results in Table II show that the double-layer PVDF sample did exhibit an increase in the voltage response compared to the single-layer sample, but with significant inefficiency, especially at higher airflow speeds. The double-layer

Journal : Large 11664 | Article No : 11097 | Pages : 18 | MS Code : 11097 | Dispatch : 29-4-2024

Table II The average of both single-layer samples, the average of the double-layer sample, the sum of the two single-layer samples, the absolute difference between the average single-layer sample's response and the double-layer sample's response, and finally, the difference between the double-layer response and the sum of the two layers AQ3

Airflow speed (km/h)	Avg of single-layer samples	Avg of double-layer sample	Sum of single-layer samples (Sample 1 + Sample 2)	(Single- + double-layer samples)	Double-layer − sum of single-layer samples
24 ± 1.5	105.429	130.857	210.857	25.429	80.00
21 ± 1.5	79.571	114.286	159.143	34.714	44.857
18 ± 1.5	75.429	99.714	150.857	24.286	51.143
15 ± 1.5	52.857	84.286	105.714	31.429	21.429
12 ± 1.5	43.714	79.143	87.429	35.429	8.286
9 ± 1.5	35.286	73.429	70.571	38.143	−2.857
6 ± 1.5	18.857	64.857	37.714	45.00	−27.143

sample had greater voltage outputs than the sum of the two individual sample's voltages until the speed reached 12 ± 1.5 m/s, after which the sum of the two samples continued to increase compared to the double-layer sample. The absolute difference between the two samples also shows a steady decrease as the speed increases, which again shows that at higher speeds, the use of two layers instead of one becomes less efficient.

Conclusion

In this work, PVDF electrospun nanofibers with good morphology, optical activity, beta sheet content, and piezo activity were fabricated at optimized experimental conditions. The feeder-to-collector distance was varied from 12 cm to 15 cm, and the generated nanomats clearly demonstrated the developmental stages of nanofiber membranes from a thin cast-like film. Film-like behavior was exhibited by the 12 cm electrospun membrane, and the increase in distance from 13 cm to 15 cm clearly showed the generation of fiber-like nanostructures, with a final successful nanofiber mat generation at the 15 cm distance. Appreciable optical activity was observed using a UV–Vis spectrophotometer, and the result clearly demonstrated a trade-off between piezoresponse and transparency. The best piezo membrane exhibited the lowest transmittance, and the transparent sample showed weak piezo activity. The beta sheet contents were calculated and found to be in the range of 69% to 78.7%. Mechanical disturbances in the form of variable forces, frequency, and impulse loading on the most efficient sample generated a maximum of 4.5 V potential, which clearly revealed the potential of PVDF nanomats in the field of energy harvesting. The dependence of the piezo potential on the resistance loads was explored using power density measurements, and a Lorentzian curve-based graphical plot was obtained for the 15 cm sample with a maximum of 21 $\mu W/m^2$, while the other sheets exhibited random behavior. The possibility of applying this efficient nanosheet in energy harvesting and sensing disciplines was studied by applying disturbances in the form of mechanical shocks by variable momentum via loads and varying airflow speeds. Energy harnessing and sensing behavior of the nanomats was tested for single- and double-layer samples, and the piezo effect was found to be enhanced with a double layer. A clear enhancement in airflow sensing efficiency was also shown by the wind-based studies for the double-layer sample, paving the way for application in complex systems for detecting gas leakages. Thus, a detailed analysis based on electrospun PVDF-based nanosheets was performed, and their potential in the field of ambient energy harvesting and sensing was thoroughly studied.

Acknowledgments This research work has been funded by a research grant received by the British Embassy in Kuwait and Foreign, Commonwealth, and Development Office (FCDO) according to the project code (PUR 1035037).

Author Contributions All authors contributed to the study conception and design. Material preparation, data collection and analysis were performed by Remya Nair, Omar Amjad, Jaffer Mehdi and Kareem Maree under the main supervision of Nader Shehata. The first draft of the manuscript was written by Ms. Remya Nair, and all authors commented on previous versions of the manuscript. The review and editing of the manuscript was performed by Ankur Jain, Ahmed Al-Dubai, Suha Jaradat, Islam Shyha, Mohamed Trabelsi, Basil Al Othman and Nader Shehata. Nader Shehata is the main supervisor and Principal Investigator of the funded grant. All authors read and approved the final manuscript.

Data availability Data are available based upon a request sent by email to the corresponding author.

Conflict of interest No potential conflicts of interest was reported by the authors.

References

1. Y. Dahman, H.H. Lo, and M. Edney, *Nanotechnology and Functional Materials for Engineers*. ed. Y. Dahman (Amstedam: Elsevier, 2017), p. 1.
2. M. Nasrollahzadeh, S.M. Sajadi, M. Sajjadi, and Z. Issaabadi, *Interface Science and Technology*. ed. M. Nasrollahzadeh, M.

Sajadi, M. Sajjadi, Z. Issaabadi, and M. Atarod (Amstedam: Elsevier, 2019), p. 1.
3. D.T. Dan, Nanotechnology, nanoparticles and nanoscience: a new approach in chemistry and life sciences. *Soft Nanosci. Lett.* 10, 17 (2020).
4. M. Rafique, M.B. Tahir, M.S. Rafique, N. Safdar, and R. Tahir, *Nanotechnology and Photocatalysis for Environmental Applications*. ed. M.B. Tahir, M. Rafique, and M.S. Rafique (Amstedam: Elsevier, 2002), p. 27.
5. J. Jeevanandam, A. Sundaramurthy, V. Sharma, C. Murugan, K. Pal, M. Kodous, and M. Danquah, *Sustainable Nanoscale Engineering*. ed. G. Szekely, and A. Livingston (Elsevier Inc., 2019), p. 83.
6. A. Al-Abduljabbar and I. Farooq, Electrospun polymer nanofibers: processing, properties, and applications. *Polym. MDPI* 15, 65 (2023).
7. H. Niu, H. Zhou, and H. Wang, *Energy Harvesting Properties of Electrospun Nanofibers*. ed. J. Fang, and T. Lin (IOP Publishing, 2019), p. 1.
8. A. Eatemadi, H. Daraee, N. Zarghami, H.M. Yar, and A. Akbarzadeh, Nanofiber: synthesis and biomedical applications. *Artif. Cells Nanomed. Biotechnol.* 44, 111 (2016).
9. J. Xue, T. Wu, Y. Dai, Y. Xia, U. States, and U. States, Electrospinning and electrospun nanofibers: methods, materials and applications. *Chem. Rev.* 119, 5298 (2019).
10. P. Lu and B. Ding, Applications of electrospun fibers. *Recent Pat. Nanotechnol.* 2, 169 (2008).
11. S. Gee, B. Johnson, and A.L. Smith, Optimizing electrospinning parameters for piezoelectric PVDF nanofiber membranes. *J. Membr. Sci.* 563, 804 (2018).
12. M. Smith and S. Kar-Narayan, Piezoelectric polymers: theory, challenges and opportunities. *Int. Mater. Rev.* 67, 65 (2022).
13. A. Toprak and O. Tigli, Piezoelectric energy harvesting: State of the art and challenges. *Appl. Phys. Rev.* 1, 031104 (2014).
14. S. Mohammadpourfazeli, S. Arash, A. Ansari, S. Yang, K. Mallick, and R. Bagherzadeh, Future prospects and recent developments of polyvinylidene fluoride (PVDF) piezoelectric polymer; fabrication methods, structure, and electro-mechanical properties. *RSC Adv. R. Soc. Chem.* 13, 370 (2023).
15. L. Persano, S.K. Ghosh, and D. Pisignano, Enhancement and function of the piezoelectric effect in polymer nanofibers. *Acc Mater Res.* 3, 900 (2022).
16. H.S. Kim, J.H. Kim, and J. Kim, A review of piezoelectric energy harvesting based on vibration. *Int. J. Precis. Eng. Manuf.* 12, 1129 (2011).
17. K.K. Sappati and S. Bhadra, Piezoelectric polymer and paper substrates: a review. *Sensors* 18, 3605 (2018).
18. S. Fotouhi, R. Akrami, K. Ferreira-Green, G.A.M. Naser, M. Fotouhi, and C. Fragassa, in *IOP Conference Series: Materials Science and Engineering* (Institute of Physics Publishing, 2019), p. 012085.
19. S. Ebnesajjad, *Introduction to Fluoropolymers, Materials Technology and Applications*. ed. S. Ebnesajjad (William Andrew and Publishing, Elsevier, 2013), p. 63.
20. R.P. Vijayakumar, D.V. Khakhar, and A. Misra, Studies on α to β phase transformations in mechanically deformed PVDF films. *J. Appl. Polym. Sci.* 117, 3491 (2010).
21. S. Mishra, L. Unnikrishnan, S.K. Nayak, and S. Mohanty, *in Macromolecular Materials and Engineering* (Wiley-VCH Verlag, 2019).
22. G. Kalimuldina, N. Turdakyn, I. Abay, A. Medeubayev, A. Nurpeissova, D. Adair, and Z. Bakenov, A review of piezoelectric PVDF film by electrospinning and its applications. *Sensors* 20, 5214 (2020).
23. S. Sukumaran, S. Chatbouri, D. Rouxel, E. Tisserand, F. Thiebaud, and T. Ben Zineb, Recent advances in flexible PVDF based piezoelectric polymer devices for energy harvesting applications. *J. Intell. Mater. Syst. Struct.* 32, 746 (2021).
24. S. Tiwari, A. Gaur, C. Kumar, and P. Maiti, Enhanced piezoelectric response in nanoclay induced electrospun PVDF nanofibers for energy harvesting. *Energy* 171, 485 (2019).
25. S. Li, A. Crovetto, Z. Peng, Ai. Zhang, O. Hansen, M. Wang, X. Li, and F. Wang, Bi-resonant structure with piezoelectric PVDF films for energy harvesting from random vibration sources at low frequency. *Sens. Actuators A* 47, 547 (2016).
26. A. Lund, K. Rundqvist, E. Nilsson, L. Yu, B. Hagström, and C. Müller, Energy harvesting textiles for a rainy day: woven piezoelectrics based on melt-spun PVDF microfibres with a conducting core. *npj Flex. Electron.* 2, 9 (2018).
27. D. Vatansever, R.L. Hadimani, T. Shah, and E. Siores, An investigation of energy harvesting from renewable sources with PVDF and PZT. *Smart Mater. Struct.* 20, 055019 (2011).
28. Y. Wang, X. Zhu, T. Zhang, S. Bano, H.P.L. Qi, Z. Zhang, and Y. Yuan, A renewable low-frequency acoustic energy harvesting noise barrier for high-speed railways using a Helmholtz resonator and a PVDF film. *Appl. Energy* 230, 52 (2018).
29. S.P. Beeby, M.J. Tudor, and N.M. White, Energy harvesting vibration sources for microsystems applications. *Meas. Sci. Technol.* 17, 175 (2006).
30. F. Hu, Q. Cai, F. Liao, M. Shao, and S.T. Lee, Recent advancements in nanogenerators for energy harvesting. *Small* 11, 5611 (2015).
31. H. Gu, Y. Zhao, and M.L. Wang, A wireless smart PVDF sensor for structural health monitoring. *Adv. Sens. Health Monit.* 12, 329 (2005).
32. S. Choi and Z. Jiang, A novel wearable sensor device with conductive fabric and PVDF film for monitoring cardiorespiratory signals. *Sens. Actuators A* 128, 317 (2006).
33. M. Tanaka, Y. Tanaka, and S. Chonan, Measurement and evaluation of tactile sensations using a PVDF sensor. *J. Intell. Mater. Syst. Struct.* 19, 35 (2008).
34. H. Luo and S. Hanagud, PVDF film sensor and its applications in damage detection. *J. Aerosp. Eng.* 12, 23 (1999).
35. C. Preusche, T. Ortmaier, and G. Hirzinger, Teleoperation concepts in minimal invasive surgery. *Control. Eng. Pract.* 10, 1245 (2002).
36. S. Sokhanvar, M. Packirisamy, and J. Dargahi, A multifunctional PVDF-based tactile sensor for minimally invasive surgery. *Smart Mater. Struct.* 16, 989 (2007).
37. L. Seminara, M. Capurro, P. Cirillo, G. Cannata, and M. Valle, Electromechanical characterization of piezoelectric PVDF polymer films for tactile sensors in robotics applications. *Sens. Actuators A Phys.* 169, 49 (2011).
38. M. Shikida, T. Shimizu, K. Sato, and K. Itoigawa, Active tactile sensor for detecting contact force and hardness of an object. *Sens. Actuators A Phys.* 103, 213 (2011).
39. Y. Bian, R. Liu, and S. Hui, Fabrication of a polyvinylidene difluoride fiber with a metal core and its application as directional air flow sensor. *Funct. Mater. Lett.* 09, 1650001 (2016).
40. Hu. Jie, H. Peng, T. Mao, T. Liu, M. Guo, Lu. Penghui, Y. Bai, and C. Zhao, An airflow sensor array based on polyvinylidene fluoride cantilevers for synchronously measuring airflow direction and velocity. *Flow Meas. Instrum.* 67, 166 (2019).
41. Y. Bian, R. Liu, X. Huang, J. Hong, H. Huang, and S. Hui, Design and fabrication of a metal core PVDF fiber for an air flow sensor. *Smart Mater. Struct.* 24, 105001 (2015).
42. R.B. Berry, G.L. Koch, S. Trautz, and M.H. Wagner, Comparison of respiratory event detection by a polyvinylidene fluoride film airflow sensor and a pneumotachograph in sleep apnea patients. *Chest* 128, 1331 (2005).

43. M. Kryger, T. Eiken, and L. Qin, The use of combined thermal/pressure polyvinylidene fluoride film airflow sensor in polysomnography. *Sleep Breath* 17, 1267 (2013).
44. K. Castkova, J. Kastyl, D. Sobola, J. Petrus, E. Stastna, D. Riha, and P. Tofel, Structure–properties relationship of electrospun pvdf fibers. *Nanomaterials* 10, 1221 (2020).
45. A.M. Ismail, M.I. Mohammed, and S.S. Fouad, Optical and structural properties of polyvinylidene fluoride (PVDF)/reduced graphene oxide (RGO) nanocomposites. *J. Mol. Struct.* 1170, 51 (2018).
46. J.C. Sampson, S. Palwai, A. Batra, and A. Vaseashta, Dielectric parametric study in electrospun PLZT/PVDF nanocomposite membranes. *Nano Tech Appl.* 5, 1 (2022).
47. H. Shao, H. Wang, Y. Cao, X. Ding, R. Bai, H. Chang, J. Fang, X. Jin, W. Wang, and T. Lin, Single-layer piezoelectric nanofiber membrane with substantially enhanced noise-to-electricity conversion from endogenous triboelectricity. *Nano Energy* 89, 106427 (2021).
48. Y. Xiao, H. Luo, R. Tang, and J. Hou, Preparation and applications of electrospun optically transparent fibrous membrane. *Polymers* 13, 506 (2021).
49. T. Blachowicz and A. Ehrmann, Optical properties of electrospun nanofiber mats. *Membranes* 13, 441 (2023).
50. C.-L. Liang, Z.-H. Mai, Qi. Xie, R.-Y. Bao, W. Yang, B.-H. Xie, and M.-B. Yang, Induced formation of dominating polar phases of poly(vinylidene fluoride): positive ion-CF_2 Dipole or Negative Ion-CH_2 dipole interaction. *J. Phys. Chem. B* 118, 9104 (2014).
51. S. Jana, S. Garain, S. Sen, and D. Mandal, The influence of hydrogen bonding on the dielectric constant and the piezoelectric energy harvesting performance of hydrated metal salt mediated PVDF films. *Phys. Chem. Chem. Phys.* 17, 17429 (2015).
52. N. Shehata, E. Elnabawy, M. Abdelkader, A.H. Hassanin, M. Salah, R. Nair, and A. Bhat, Static-aligned piezoelectric poly (Vinylidene Fluoride) electrospun nanofibers/MWCNT composite membrane: facile method. *Polymers* 10, 965 (2018).
53. Z. Zhao, J. Li, X. Yuan, X. Li, Y. Zhang, and J. Sheng, Preparation and properties of electrospun poly(vinylidene fluoride) membranes. *J. Appl. Polym. Sci.* 97, 466 (2005).
54. B. Azimi, M. Milazzo, A. Lazzeri, S. Berrettini, M.J. Uddin, Z. Qin, M.J. Buehler, and S. Danti, Electro–spinning piezoelectric fibers for biocompatible devices. *Adv. Healthc. Mater.* 9, 1 (2020).
55. K.H. Lee, H.Y. Kim, H.J. Bang, Y.H. Jung, and S.G. Lee, The change of bead morphology formed on electrospun polystyrene fibers. *Polymer* 44, 4029 (2003).
56. K. AnjiReddy and S. Karpagam, Chitosan nanofilm and electrospun nanofiber for quick drug release in the treatment of Alzheimer's disease: in vitro and in vivo evaluation. *Int. J. Biol. Macromol.* 105, 131 (2017).
57. N.S.A. Rahman, Y.E. Greish, S.T. Mahmoud, N.N. Qamhieh, F. El-Maghraby, and D. Zeze, Fabrication and characterization of cellulose acetate-based nanofibers and nanofilms for H_2S gas sensing application. *Carbohydr. Polym.* 258, 117643 (2021).
58. X. Hu, M. You, N. Yi, X. Zhang, and Y. Xiang, Enhanced piezoelectric coefficient of PVDF- TrFE films via in situ polarization. *Front. Energy Res.* 9, 621540 (2021).

Journal:	**11664**
Article:	**11097**

Author Query Form

Please ensure you fill out your response to the queries raised below and return this form along with your corrections

Dear Author

During the process of typesetting your article, the following queries have arisen. Please check your typeset proof carefully against the queries listed below and mark the necessary changes either directly on the proof/online grid or in the 'Author's response' area provided below

Query	Details Required	Author's Response
AQ1	Various edits were made for grammar/syntax. Please check all changes to ensure that the correct intent has been preserved, and amend wherever necessary.	
AQ2	Journal instruction requires a city for affiliations; however, these are missing in affiliation [1]. Please verify if the provided city is correct and amend if necessary.	
AQ3	The caption description (absolute difference between the average single-layer sample's response and the double-layer sample's response) in Table II doesn't seem to match the heading for column 5 in the table. Please check.	